Localization, antilocalization, and delocalization in one-dimensional disordered lattices

J. Heinrichs
Institut de Physique B5, Université de Liège, Sart Tilman, B-4000 Liège, Belgium
(Received 27 July 1994)

We study analytically the eigenstates of a weakly disordered semi-infinite single-band tight-binding lattice in contact with an ordered parent lattice. We consider successively three simple types of correlated, continuously distributed site energies: a random dimer model, a random trimer model, and a random monomer-dimer model. In the dimer model the disordered chain lattice is partitioned into a collection of pairs of nearest-neighbor sites, where the two sites of a given pair are assigned a common independent random energy. The trimer model is similarly made up of triplets of nearest-neighbor sites having the same site energy taken as an independent random variable. Finally, the monomer-dimer model is defined as an alternate sequence of independent dimers and monomers with identically distributed site energies. The site energy randomness is described by Gaussian white noise and we restrict to energies of the pure system's energy band. We find that the averaged rates of exponential variation of site wave functions at finite distances $N \gg 1$ from the edge site of the disordered chain are anomalous at the band center ($E=0$), at the band edges, and at energies $E=2\cos\alpha\pi$, with $\alpha=\frac{1}{4}$ for the dimer model and $\alpha=\frac{1}{6}$ $\frac{1}{3}$, $\frac{2}{3}$, and $\frac{5}{6}$ for the trimer and monomer-dimer models. These results are relevant for transport behavior of finite disordered samples in the quasimetallic regime. On the other hand, we study the inverse localization lengths for the states whose energies are intermediate to the above special values. In the dimer model all the states in this energy range are localized, with an enhanced localization length. In the trimer and monomer-dimer models we obtain six delocalized states at fixed intermediate energies. The energies of the delocalized states separate domains where all states are localized from domains where all states are antilocalized. The antilocalized states discussed in this paper have the usual Bloch form up to the edge site of the ordered lattice, beyond which they decrease exponentially into the disordered lattice. We also study the effect of disorder on the phase of site wave functions.

I. INTRODUCTION

In a recent paper[1] (hereafter referred to as I) we have studied analytically the rates of exponential variation of site wave functions as a function of the distance from the edge in a semi-infinite disordered chain lattice in contact with a semi-infinite nondisordered lattice. In the usual single-band tight-binding approximation the system consists of a semi-infinite disordered chain with sites $n=1,2,3,\ldots$ having random site energies, which is adjacent to a semi-infinite nondisordered chain with sites $n=0,-1,-2,\ldots$ whose energy level is placed at the zero of energy. Taking the constant hopping rate between nearest neighbors to be the same for the two chains, the Schrödinger equation for site wave functions of energy E (in units of the hopping rate) is

$$\psi_{n+1}+\psi_{n-1}+\epsilon_n\psi_n=E\psi_n\ ,$$
$$n=0,\pm1,\pm2,\ldots;\ \epsilon_n=0\ \text{ for } n=0,-1,\ldots\ . \quad (1)$$

In I we focused on the study for weak disorder of the modification of a tight-binding plane wave when penetrating the disordered region.

The site energies at $n=1,2,3,\ldots$ were assumed to be identically distributed, uncorrelated Gaussian variables with zero mean, i.e.,

$$\langle\epsilon_n\rangle=0,\quad \langle\epsilon_n\epsilon_m\rangle=\epsilon_0^2\delta_{m,n}\ . \quad (2)$$

At the sites of the semi-infinite nondisordered chain the solutions of (1) are of the form

$$\psi_n=e^{iqn},\quad n=0,-1,-2,\ldots, \quad (3)$$

which correspond to the usual Bloch spectrum

$$E=2\cos q \quad (4)$$

and define the boundary conditions

$$\psi_0=1,\quad \psi_1=e^{iq} \quad (5)$$

for the site wave functions at energies within the band (4) in the disordered region, which are obtained by iterating (1) starting from the edge site $n=1$.

The random complex rate of exponential variation of the amplitude ψ_N, $N-1\sim N$ steps away from the edge site in the disordered lattice is defined by

$$\gamma_N=N^{-1}\ln\psi_N\ . \quad (6)$$

In the asymptotic limit $1\ll N\to\infty$, γ_N is self-averaging (Fürstenberg's theorem) and independent of N, i.e., it has a well-defined stationary central value which is equal to the disorder average

$$\langle\gamma\rangle=\lim_{N\to\infty}N^{-1}\langle\ln\psi_N\rangle\ . \quad (7)$$

Its real part (the Lyapounov exponent), which is found to

be positive for uncorrelated site energies, defines the inverse localization length

$$\xi^{-1} \equiv \mathrm{Re}\langle \gamma \rangle = \lim_{N \to \infty} N^{-1} \langle \ln \psi_N \rangle \ . \tag{8}$$

The imaginary part of (6) corresponds to oscillations of the wave functions about exponentially growing (or decreasing) amplitudes, which are not directly related to the density of states for the ordered lattice-disordered lattice junction described by (1), unlike the corresponding quantity in the case of a finite disordered chain placed in vacuum.

In I we obtained the site wave functions in the disordered lattice for weak disorder, using an expansion in terms of contributions of successively higher orders in the site energies. For energies sufficiently far from the band center and the band edges the expansion converges for all distances N, thus allowing a straightforward determination of the inverse localization length in this case. In particular, to lowest order in the correlation parameter ϵ_0^2, the localization length reduces to the well-known result for these intermediate energies.[2] On the other hand, it was shown in I that near the band center and near the band edges, the validity of the weak disorder expansion is restricted to scales N which are somewhat less than the localization length and, furthermore, that the averaged exponential rates $\langle \gamma_N \rangle$ take on anomalous forms. The length dependence of the site wave functions ψ_N at these scales is relevant for the study of quasimetallic transport in finite samples of lengths $N \ll \xi$. We also note that the averages $\mathrm{Re}\langle \gamma_N \rangle$ and $\mathrm{Im}\langle \gamma_N \rangle$ properly reflect the statistical behavior of γ_N since it was shown in I that γ_N remains self-averaging for finite N provided $N \gg 1$.

An important recent development in the theory of disordered tight-binding lattices has been the explicit demonstration of the existence of delocalized states in models involving a specific type of correlation of the random site energies known as random dimer models. This was first shown by Dunlap, Kundu, and Phillips[3] and by Dunlap, Wu, and Phillips[4] and subsequently by many others.[5–13] In the random dimer model of Dunlap *et al.*[3,4] the sites of a chain of $2N$ sites are arbitrarily grouped into N pairs of nearest-neighbor sites (dimers) and are assigned at random one of two values of site energies (ϵ_A or ϵ_B) with the restriction that the two members of any dimer are assigned the same energy. This contrasts with the model of I where the energy of every site of the disordered chain is taken to be an independent, continuous random variable described by (2). Dunlap *et al.*, found that the random dimer model has $2\sqrt{N}$ delocalized states.[3] Since these states constitute a subset of measure zero the familiar theorem about localization in one-dimensional disordered systems is preserved in the presence of the dimer correlation. The model of Dunlap *et al.*[3,4] has been generalized in studies of delocalized states for cases where the sites of a disordered chain are grouped into n-mer units[7,12] comprising n sites in succession, all of which are assigned a common random site energy.

The previous studies of delocalized states in one-dimensional disordered systems are restricted essentially to discrete distributions of site energies, namely the double-valued distribution used by Dunlap *et al.*[3,4] The purpose of this paper is to generalize the analytical study of localization in the ordered-disordered lattice system above[1] in the presence of various multimer correlations with continuously distributed site energies. More precisely, the common site energy for the sites of a multimer will be taken to be an independent random variable described by a Gaussian white-noise correlation of the form (2) for different multimers units. We shall consider successively three distinct random models: a dimer model, a trimer model, and a mixed model of alternating dimers and monomers (single-site units).

In Sec. II, after recalling some general results leading to the weak disorder expansion of the rates of exponential variation of site wave functions for finite N, we derive the detailed analytical form of $\langle \gamma_N \rangle$ to linear order in ϵ_0^2 for arbitrary energies (4), successively for the three random multimer models above. In Sec. III,, we study the explicit results for the anomalous forms of the site-wave-function rates $\langle \gamma_N \rangle$ at finite distances N, at special energies defined in Sec. II, together with the localization lengths of the states of energies intermediate to these special values. Some concluding remarks are presented in Sec. IV.

II. WEAK DISORDER EXPANSION OF WAVE FUNCTIONS

A. General expressions

We first recall some general results of I for the site wave functions in the disordered region before defining multimer correlations of site energies as mentioned in Sec. I. For energies E within the pure system's band (4) the wave functions in the disordered lattice are written in the form[1]

$$\psi_n = e^{iqn + if_n} \ , \tag{9}$$

where the local exponent increments,

$$g_n = f_n - f_{n-1} \ , \tag{10}$$

are given by a two-point recursion relation which follows from (1).[1] For weak disorder the g_n are defined in terms of contributions of successive orders in the site energies ϵ_n,

$$g_n = \sum_{p=1,2,3,\ldots} g_n^{(p)}, \quad g_n^{(p)} = f_n^{(p)} - f_{n-1}^{(p)} \ , \tag{11}$$

where the pth order contribution, $g_n^{(p)}$, is given by a recursion relation obtained by equating the terms of pth order on both sides of the expansion of the equation for g_n in terms of successively higher contributions in the ϵ_n. The explicit solutions of the recursion relations for $g_n^{(1)}$ and $g_n^{(2)}$, using the boundary conditions (5), are[1]

$$g_n^{(1)} = ib \sum_{m=1}^{n-1} \epsilon_m a^{n-m-1} \ , \tag{12}$$

$$g_n^{(2)} = \sum_{m=1}^{n-1} \Gamma_m a^{n-m-1} \ , \tag{13}$$

where

$$a=e^{-2iq},\quad b=e^{-iq}, \tag{14}$$

and

$$\Gamma_m=\frac{i\epsilon_m^2 a}{2}+\epsilon_m b^3 g_m^{(1)}-\frac{ia}{2}(1+a)g_m^{(1)2}. \tag{15}$$

From (6) and (9) we then have $\gamma_N=iq+iN^{-1}f_N$, and by iterating (10), starting from the values

$$f_1=g_1=0 \tag{16}$$

[Eq. (5)] we get

$$\gamma_N=iq+\frac{i}{N}\sum_{n=1}^{N}\sum_{p} g_n^{(p)}\equiv iq+\gamma_N^{(1)}+\gamma_N^{(2)}+\cdots, \tag{17}$$

where, from (2), $\langle\gamma_N^{(2p+1)}\rangle=0$. In I it was shown that γ_N is self-averaging for all $N\gg1$, when the energies at all the sites are uncorrelated. We expect this also to be the case for the various multimer models discussed below. Therefore we shall restrict ourselves in the following to the study of the mean $\langle\gamma_N\rangle$, keeping in mind that the results will be significant only for $N\gg1$. Expressions (12)–(15) allow us to study the complex mean $\langle\gamma_N\rangle$ to lowest order in the disorder, i.e., $\langle\gamma_N\rangle=iq+\langle\gamma_N^{(2)}\rangle$. In particular, the study of $\langle\gamma_N\rangle$ will enable us to find the localization length for intermediate band energies alluded to earlier.

B. Random dimer model

We now arrange the sites $n=1,2,3,\ldots$ in the disordered region into pairs (1,2), (3,4), (5,6), . . . of neighboring sites and we choose the site energies of the two members of a pair to be equal, that is we put $\epsilon_1=\epsilon_2\equiv\epsilon_1$, $\epsilon_3=\epsilon_4\equiv\epsilon_3,\ldots$, where the site energies on different pairs are uncorrelated Gaussian variables defined by (2). For this random dimer model Eq. (12) becomes

$$g_m^{(1)}=iba^{m-1}\left[\sum_{p=0}^{k-1}\epsilon_{2p+1}(a^{-(2p+1)}+a^{-2(p+1)})(\delta_{m,2k+1}+\delta_{m,2(k+1)})+\epsilon_{m-1}a^{-m+1}\delta_{m,2(k+1)}\right], \tag{18}$$

where the different forms of $g_m^{(1)}$ for even and odd labeled sites m are shown explicitly. It thus follows that Γ_m also has different forms for even and odd m and that furthermore the form of $\langle\gamma_N^{(2)}\rangle$ depends on whether the length N corresponds to an integer number of dimers in succession or not. With this in mind, we obtain from (13), (15), (18), and (2)

$$\begin{aligned}\langle\gamma_N^{(2)}\rangle=iq+i\left[\frac{\delta_{N,2M}}{2M}+\frac{\delta_{N,2M+1}}{2M+1}\right]\sum_{l=1}^{M}\Bigg[&(1+a)\langle\Gamma_{2l-1}\rangle+\langle\Gamma_{2l}\rangle\\&+(1+a^{-1})a^{2l}\sum_{k=0}^{l-2}(\langle\Gamma_{2k+1}\rangle a^{-(2k+1)}+\langle\Gamma_{2(k+1)}\rangle a^{-2(k+1)})\Bigg]\\&-i\frac{a^{2M}}{2M}\delta_{N,2M}\sum_{k=0}^{M-1}(\langle\Gamma_{2k+1}\rangle a^{-(2k+1)}+\langle\Gamma_{2(k+1)}\rangle a^{-2(k+1)}),\end{aligned} \tag{19}$$

where

$$\langle\Gamma_m\rangle=\frac{i\epsilon_0^2 a}{2}[1+a(3+a)\delta_{m,2(k+1)}+(1+a)^3(a^4-1)^{-1}(1-a^{-4k})a^{2m-1}(\delta_{m,2k+1}+\delta_{m,2(k+1)})]. \tag{20}$$

The summation of the various geometric series involved in (18) and (19) yields, after some calculations and reductions of terms,

$$\begin{aligned}\langle\gamma_N^{(2)}\rangle=\frac{-\epsilon_0^2 a}{2(a-1)^2}\Bigg\{&(1+a)\left[\delta_{N,2M}+\frac{\delta_{N,2M+1}}{1+(2M)^{-1}}\right]\\&+ia[a(1+a)^2S_M^{(4)}-2(1+3a)S_M^{(2)}]\left[\frac{S_{N,2M}}{2M}+\frac{\delta_{N,2M+1}}{2M+1}\right]\\&+\frac{\delta_{N,2M}}{2M}\left[-(a-1)^2(1+4a+a^2)S_M^{(2)}+\frac{(a+1)^2a^{2M}}{1+a^2}(1+a^2-a^{2M}-a^{-2M+2})\right]\Bigg\},\end{aligned} \tag{21}$$

where

$$S_M^{(k)}=\frac{1-a^{kM}}{1-a^k} \tag{22}$$

denotes a geometric sum, which is finite for any a, for finite M.

Equation (21) leads to the identification of various domains within the energy band (4) where distinct behavior is to be expected for $\langle\gamma_N^{(2)}\rangle$. Indeed, consider the set of special energies at which the sum $S_M^{(k)}$ with the

highest index k, namely $S_M^{(4)}$, increases linearly with M. These energies are defined by the roots $a=\pm 1$ and $a=\pm i$ of

$$a^4=1\ ,$$

i.e.,

$$E=0 \quad \left[q=\frac{\pi}{2}\right]\ ,$$

$$E=\pm 2 \quad (q=0,\pi)\ , \tag{23}$$

and

$$E=\pm\sqrt{2} \quad \left[q=\frac{\pi}{4},\frac{3\pi}{4}\right]\ ,$$

which corresponds to the band center, the band edges, and the energies at the rational values $q/\pi=\frac{1}{4}$ and $\frac{3}{4}$, respectively. At all other energies of the band $S_M^{(4)}$ and $S_M^{(2)}$ are finite for all M and the curly bracket in (21) reduces to just the term independent of M for $M\to\infty$. However, at the special energies above, the M-dependent terms in (21) may lead to contributions of the same order as the terms which are independent of M, as a result of the linear variation of $S_M^{(k)}$ with M.

This shows that the detailed forms of $\langle\gamma_N^{(2)}\rangle$ at the various characteristic energies above will generally be different. This is the case, in particular, at the band edges (where both $S_M^{(4)}$ and $S_M^{(2)}$ grow linearly with M) and at the energies $E=\pm\sqrt{2}$ (where only $S_M^{(4)}$ varies linearly), respectively. In fact, the special energies above ($E=\pm 2$, $E=+-\sqrt{2}$, $E=0$) define energy domains (the neighborhood of the band edges, of the band center, and of energies $\pm\sqrt{2}$) where $\langle\gamma_N^{(2)}\rangle$ takes special (anomalous) forms as compared to its form at intermediate energies, i.e., energies sufficiently far removed from these special values. Furthermore, among the domains of anomalous behavior for $\langle\gamma_N^{(2)}\rangle$ the neighborhood of the band edges plays a distinct role. Indeed, the anomalies are expected to be enhanced near the band edges because of the double pole at $a=1$ appearing in the overall factor of (21). Due to the fact that for finite N $\langle\gamma_N^{(2)}\rangle$ is, however, a finite quantity, this second-order pole must be cancelled by a corresponding double root in the curly bracket. This feature renders $\langle\gamma_N^{(2)}\rangle$ strongly N dependent near the band edges, unlike at the other special energies.

On the other hand, at the above special energies the weak disorder expansion, of which (21) is the lowest term, is expected to converge only for N less than a threshold value of the order or smaller than the localization length. This has been shown in our earlier study[1] of the tight-binding model, where the site energies at all the sites are uncorrelated (monomer model), by analyzing the detailed form of the next-to-leading contribution to the rate of variation of the wave functions.

The anomalies of $\langle\gamma_N^{(2)}\rangle$ for finite N at the special energies are the analog of the well-known Kappus-Wegner and Derrida-Gardner anomalies of the inverse localization length in the stationary ($N\to\infty$) limit.[14,15] Their detailed discussion for the dimer model, from Eq. (21), is given in Sec. III. For intermediate energies where the weak disorder expansion for $\langle\gamma_N\rangle$ converges we shall obtain the localization length from the stationary limit of (21) for $N\to\infty$.

C. Random trimer model

Here the sites $n=1,2,3,\ldots$ in the disordered region are grouped into triplets (1,2,3), (4,5,6), (7,8,9), ... of neighboring sites in succession, with the three members of a triplet having the same site energy in any realization. Again the site energies on distinct triplets are assumed to be identically (continuously) distributed independent random variables described by correlation (2).

At present one has to distinguish between three cases in determining $g_m^{(1)}$ and the inhomogeneous term Γ_m in the recursion relation for $g_m^{(2)}$: the case where m is an integer multiple $(k+1)$ of 3, and the cases $m=3k+2$ and $m=3k+1$. By decomposing the summation in (13) in terms of these three types of terms one obtains for the average of $\gamma_N^{(2)}$ in (17), e.g., for $N=3M+1$,

$$\begin{aligned}\langle\gamma_{3M+1}^{(2)}\rangle=i(3M+1)^{-1}\Bigg\{&\sum_{l=0}^{M}a^{3l}\sum_{k=0}^{l-1}(\langle\Gamma_{3k+1}\rangle a^{-(3k+1)}+\langle\Gamma_{3k+2}\rangle a^{-(3k+2)}+\langle\Gamma_{3(k+1)}\rangle a^{-3(k+1)})\\&+\sum_{l=1}^{M}a^{3l-1}\Bigg[\langle\Gamma_{3l-1}\rangle a^{-(3l-1)}+\langle\Gamma_{3l-2}\rangle a^{-(3l-2)}\\&\quad+\sum_{k=0}^{l-2}(\langle\Gamma_{3k+1}\rangle a^{-(3k+1)}+\langle\Gamma_{3k+2}\rangle a^{-(3k+2)}+\langle\Gamma_{3(k+1)}\rangle a^{-3(k+1)})\Bigg]\\&\quad+\sum_{l=1}^{M}a^{3l-2}\Bigg[\langle\Gamma_{3l-2}\rangle a^{-(3l-2)}\\&\qquad+\sum_{k=0}^{l-2}(\langle\Gamma_{3k+1}\rangle a^{-(3k+1)}+\langle\Gamma_{3k+2}\rangle a^{-(3k+2)}\\&\qquad+\langle\Gamma_{3(k+1)}\rangle a^{-3(k+1)})\Bigg]\Bigg\}\ .\end{aligned} \tag{24a}$$

By separating out the term $k=l-1$ in the summand of the first double sum in the curly bracket of (24a) the expressions for $\langle\gamma_{3M}^{(2)}\rangle$, $\langle\gamma_{3M-1}^{(2)}\rangle$ may be conveniently written as

$$\langle\gamma_{3M}^{(2)}\rangle=[1+(3M)^{-1}]\langle\gamma_{3M+1}^{(2)}\rangle-i(3M)^{-1}a^{3M}\sum_{k=0}^{M-1}(\langle\Gamma_{3k+1}\rangle a^{-(3k+1)}+\langle\Gamma_{3k+2}\rangle a^{-(3k+2)}+\langle\Gamma_{3(k+1)}\rangle a^{-3(k+1)}) \tag{24b}$$

and

$$\langle\gamma_{3M-1}^{(2)}\rangle=[1-(3M)^{-1}]^{-1}\langle\gamma_{3M}^{(2)}\rangle - i(3M-1)^{-1}\left[\langle\Gamma_{3M-1}\rangle+a\langle\Gamma_{3M-2}\rangle + a^{3M-1}\sum_{k=0}^{M-2}(\langle\Gamma_{3k+1}\rangle a^{-(3k+1)}+\langle\Gamma_{3k+2}\rangle a^{-(3k+2)}+\langle\Gamma_{3(k+1)}\rangle a^{-3(k+1)})\right] . \tag{24c}$$

Here the explicit expression of Γ_M obtained from (15), (12), and (2) is

$$\langle\Gamma_m\rangle=\frac{i\epsilon_0^2 a}{2}\left[1+a(a+3)\delta_{m,3k+2}+a(a+1)(a^2+2a+3)\delta_{m,3(k+1)} + \frac{(1+a)(1+a+a^2)^2}{a(a^6-1)}a^{2m}(1-a^{-6k})(\delta_{m,3k+1}+\delta_{m,3k+2}+\delta_{m,3(k+1)})\right] . \tag{25}$$

By inserting (25) in (24a) and performing the geometric sums we obtain, after various rearrangements and reductions of terms,

$$\langle\gamma_{3M+1}^{(2)}\rangle=-\frac{\epsilon_0^2 a}{2(3M+1)}\left\{M[2+a+a^2+(1+a)(1+6a+3a^2+a^3)] + \frac{a}{a-1}(1+4a+9a^2+4a^3+a^4)(S_M^{(3)}-M) + \frac{a(1+a+a^2)^2}{(a-1)^2}[aS_M^{(6)}-(a+1)S_M^{(3)}+M]\right\} . \tag{26a}$$

From a discussion analogous to that presented for the dimer model one concludes from (26a) that distinct types of anomalous behavior for $\langle\gamma_N^{(2)}\rangle$ exist near the following band energies:

$$E=0 \quad \left[q=\frac{\pi}{2}\right], \quad E=\pm 2 \quad (q=0,\pi), \quad E=\pm\sqrt{3} \quad \left[q=\frac{\pi}{6},\frac{5\pi}{6}\right] , \tag{27}$$

and

$$E=\pm 1 \quad \left[q=\frac{\pi}{3},\frac{2\pi}{3}\right] ,$$

which correspond to the solutions of

$$a^6=(a^2-1)(a^2+a+1)(a^2-a+1)=1 , \tag{28}$$

at which $S_M^{(6)}$ in (26a) grows linearly with M. Again the expressions for $\langle\gamma_{3M+1}^{(2)}\rangle$ at these energies discussed in Sec. III are valid in the metallic domain while the corresponding expression for intermediate energies remains valid up to $N\to\infty$, thus defining the localization length. Note that in arriving at (26a) we have exactly cancelled a denominator, $1-a+a^2$ (with zeros at $E=\pm\sqrt{3}$), which appeared, in particular, as an extra denominator in terms involving the anomalous sum $S_M^{(6)}$. The absence of such an extra denominator in (26a) shows that an enhancement of the anomaly at $E=\pm\sqrt{3}$, which would be expected from this denominator, does not exist.

Finally we turn to Eqs. (24b) and (24c) where, by using (25), we obtain successively

$$\langle\gamma_{3M}^{(2)}\rangle=[1+(3M)^{-1}]\langle\gamma_{3M+1}^{(2)}\rangle + \frac{\epsilon_0^2}{6M}a^{3M+1}\left[a^{-3}(a^4+4a^3+9a^2+4a+1)S_M^{(-3)}+\frac{(1+a+a^2)^2}{(a-1)(1-a+a^2)}(S_M^{(3)}-S_M^{(-3)})\right], \tag{26b}$$

and

$$\langle\gamma_{3M-1}^{(2)}\rangle=\frac{1}{1-(3M)^{-1}}\langle\gamma_{3M}^{(2)}\rangle + \frac{\epsilon_0^2 a}{2(3M-1)}\left[a^2(a^4+4a^3+9a^2+4a+1)S_{M-1}^{(3)}+a^2(a+1)(1+a+a^2)^2S_{M-1}^{(6)} + \frac{(1+a+a^2)^2a^{3M-1}}{(a-1)(1-a+a^2)}(S_{M-1}^{(3)}+S_{M-1}^{(-3)})+1+4a+a^2\right], \tag{26c}$$

which will be analyzed in detail at the special energies (27) in Sec. III.

D. Random dimer-monomer model

Finally, we consider a simple alternative trimerization model where we define a triplet unit composed of a dimer and of a neighboring isolated site which fluctuates independently of the dimer and of the sites of neighboring triplets. Thus we arrange the site of the sequence $n=1,2,3,4,\ldots$ into independent units [(1,2),3], [(4,5),6], [(7,8),9], ... where the constituent sites of the dimer of a given triplet are chosen to have the same site energy, while the remaining site of the triplet has an energy which fluctuates independently from that of the dimer to which it is associated. More simply, this model may thus be referred to as a random system of alternating independent dimers and monomers.

In the present case Eq. (12) has three possible forms which may be combined in the following expression:

$$g_n^{(1)}=iba^{n-1}[(h_k+s_k)(\delta_{n,3k+1}+\delta_{n,3k+2}) + (h_{k+1}+s_k)\delta_{n,3(k+1)}+\epsilon_{n-1}a^{-(n-1)}\delta_{n,3k+2}], \tag{29}$$

where

$$h_k=\sum_{p=0}^{k-1}\epsilon_{3p+1}(a^{-(3p+1)}+a^{-(3p+2)}), \tag{30}$$

$$s_k=\sum_{p=1}^{k}\epsilon_{3p}a^{-3p}. \tag{31}$$

The explicit form of Γ_m obtained from (15), (29)–(31) and (2) may be written, after some calculations, in the rather compact form

$$\langle\Gamma_m\rangle=\frac{i\epsilon_0^2}{2}(a+a^2(a+3)\delta_{m,3k+2}+(a+1)a^{2m-4}\{[(1+a)^2+a^{-2}]S_k^{(-6)}[\delta_{m,3k+1}+\delta_{m,3k+2}] + [(1+a)^2S_{k+1}^{(-6)}+a^{-2}S_k^{(-6)}]\delta_{m,3(k+1)}\}), \tag{32}$$

and the form of the rates of exponential variation of wave functions at the three distinct types of sites $N\gg1$ are defined by (24a)–(24c). Thus by evaluating the various summations over $\langle\Gamma_m\rangle$ in Eq. (24a) using (32) and (22) one obtains, with some patience,

$$\langle\gamma_{3M+1}^{(2)}\rangle=-\frac{\epsilon_0^2}{2(3M+1)}\left\{a(1+a+a^2)[M+au(S_M^{(6)}-M)] + a(a+1)\left[(1+3a+a^2)M+a^3u(S_M^{(6)}-M)+aM-\frac{a^2(a+1)}{a^6-1}(a^4+a^2+2a+1)M\right] + \frac{a^2}{a-1}\left[(a^3+4a^2+a+1)(S_M^{(3)}-M)-(a+1)u[(a^3+1)S_M^{(3)}-S_M^{(6)}-a^3M] - \frac{a^2(a+1)}{a^6-1}[(a^3+1)(a+a^{-1}+3)S_M^{(3)} - (a^4+2a^3+a^2+1)(a^4+1)S_M^{(6)}-(a+a^{-1}+3)M]\right]\right\}, \tag{33}$$

where

$$u=\frac{1}{a-1}\left[1+\frac{2a^3}{a^4+a^2+1}\right]. \tag{34}$$

From the form of (33) it follows that, like for the random trimer model, one expects anomalous behavior for $\langle\gamma_{3M+1}^{(2)}\rangle$ in the vicinity of the special energies (27) corresponding to the solutions of (28). Furthermore, due to the occurrence of terms with a denominator a^6-1 multiplying the anomalous quantities $S_M^{(6)}$ and $S_M^{(3)}$ in (33), one generally expects more pronounced anomalies than in the corresponding expression (26a) for the trimer model. Some detailed results are presented in Sec. III. Since the differences between the forms of $\langle\gamma_N^{(2)}\rangle$ for the three types of sites $3M+1$, $3M$, and $3M-1$ have already been investigated for the trimer model [Eqs. (26a)–(26c)], we refrain from discussing here the analogous but more cumbersome) expressions for $\langle\gamma_{3M}^{(2)}\rangle$ and $\langle\gamma_{3M-1}^{(2)}\rangle$ for the monomer-dimer model. Their analysis, along with other details, are deferred to a later more technical publication.[16]

III. DETAILED RESULTS

In this section we analyze the detailed form of the exponential rates of variation of wave function amplitudes at a distance N from the edge site, for the three models of correlated site energies defined in Sec. II. For intermediate energies the weak disorder expansions for $\langle\gamma_N^{(2)}\rangle$ converge to a stationary limit for $N\gg1$, from which we obtain the localization length. On the other hand, in studying anomalies of $\langle\gamma_N^{(2)}\rangle$ at finite distances $N\gg1$ we restrict for simplicity to expressions right at the special energies above, although the general results of Sec. II permit, of course, their study (with additional effort) in small neighborhoods of these energies. These further details are also deferred to the later paper.[16]

A. Dimer model

We first analyze (21) at energies sufficiently far away from the edges and from the center of the band (4). For $N\to\infty$ we then obtain

$$\langle\gamma^{(2)}\rangle\equiv\lim_{N\to\infty}\langle\gamma_N^{(2)}\rangle=-\frac{\epsilon_0^2a(1+a)}{2(a-1)^2}+O\left[\frac{1}{N}\right], \tag{35}$$

where, by using (4) and (14), we obtain

$$\mathrm{Re}\langle\gamma^{(2)}\rangle=\frac{\epsilon_0^2E^2}{4}, \tag{36}$$

$$\mathrm{Im}\langle\gamma^{(2)}\rangle=-\frac{\epsilon_0^2}{8}\sin2q. \tag{37}$$

The Eq. (36) may be compared with the weak disorder result for the inverse localization length for completely uncorrelated site energies (monomer model), namely

$$\langle\gamma^{(2)}\rangle=\frac{\epsilon_0^2}{2(4-E^2)}, \tag{38}$$

first derived by Thouless.[2] It follows that, in the dimer model, the localization length is larger than in the corresponding monomer model except at the four intermediate energy values, $E=\pm\sqrt{2\pm\sqrt{2}}$, at which they coincide. The enhancement of the localization length in the dimer case is a consequence of the reduced disorder as a result of the dimer correlation. The dimer correlation also leads to a nonvanishing imaginary part (37) in $\langle\gamma^{(2)}\rangle$ which describes a modification of the Bloch phase (3) due to the disorder. The above discussion for intermediate energies remains valid for finite $N\gg1$ to leading order in N^{-1} since, as recalled earlier, our weak disorder expansion is defined for all N in this case.

We now turn to the discussion of the form of $\langle\gamma_N^{(2)}\rangle$ at the special energies given by (23), restricting to the domain of finite $1\ll N<\xi$ for which the weak disorder expansion is nondivergent.[1] At the band center $E=0$ ($q=\pi/2$) we substitute the values $a=-1$ and $S_M^{(4)}=S_M^{(2)}=M$ in (21) which readily yields the real expression

$$\langle\gamma_N^{(2)}\rangle=\frac{\epsilon_0^2}{4}\delta_{N,2M}-\frac{\epsilon_0^2}{4}\frac{1}{1+(2M)^{-1}}\delta_{N,2M+1}, \qquad E=0. \tag{39}$$

Note that (39) differs quite drastically from the extrapolation of (36) to the band center, i.e., $\langle\gamma^{(2)}\rangle=0$. In particular (39) implies that, as a result of the site-energy correlations, the wave function at a given dimer unit at a short distance from the edge site is composed of a dominant exponentially large part at the even site and a corresponding exponentially small part at the odd site.

At the special energies $E=\pm\sqrt{2}$ ($q=\pi/4,3\pi/4$) we obtain $\langle\gamma_N^{(2)}\rangle$ for sites $N=2M+1$ by substituting the values $a=\pm i$, $S_M^{(4)}=M$, and $S_M^{(2)}=\frac{1}{2}[1-(-1)^M]$. At the even sites the indeterminacy at $a^2=-1$ which is present in the last term of the curly bracket in (21) must first be removed (by means of power series expansion in the neighborhood of $a^2=-1$). In this way we obtain successively

$$\langle\gamma_{2M}^{(2)}\rangle=\frac{\epsilon_0^2}{4}\left[(1\pm2i)-\frac{1}{2M}(1\pm3i)[1-(-1)^M]\right], \tag{40a}$$

$$\langle\gamma_{2M+1}^{(2)}\rangle=\frac{1}{4}\frac{\epsilon_0^2}{1+(2M)^{-1}}\left[1+\frac{3\mp i}{2M}[1-(-1)^M]\right], \qquad E=\pm\sqrt{2}, \tag{40b}$$

where expressions with the upper sign apply for $E=\sqrt{2}$ and those with the lower sign for $E=-\sqrt{2}$. We note that at the distances of interest ($N\gg1$) the real parts of the expressions (40a) and (40b) for the two types of sites differ only by terms of $O(1/M)$, unlike the corresponding expression (39) at the band center.

Finally, we study the form of $\langle\gamma_N^{(2)}\rangle$ at the band edges ($a=1$), where the whole expression (21) is indeterminate due to the overall factor $(a-1)^{-2}$. From an expansion of (21) to leading order in small deviations from the value $a=1$, we obtain the following results in final form:

$$\langle \gamma_{2M}^{(2)} \rangle = -\frac{4\epsilon_0^2 M^2}{3}\left[1-\frac{9}{8M}+\frac{5}{16M^2}\right], \tag{41a}$$

$$\langle \gamma_{2M+1}^{(2)} \rangle = -\frac{4\epsilon_0^2}{3}\frac{M^2}{1+(2M)^{-1}}\left[1+\frac{3}{8M}-\frac{1}{16M^2}\right], \quad E=\pm 2 . \tag{41b}$$

Apart from the strong length dependence of these rates their most remarkable feature is their negative sign, which implies a phenomenon of antilocalization at short distances at the band edges: at these energies an incident Bloch wave at the edge site of the semi-infinite disordered chain decreases exponentially as it penetrates inside the chain. This is to be contrasted, e.g., with the positive value of $\langle \gamma_N^{(2)} \rangle$ for finite N at intermediate energies at which the wave functions thus tend to localize away from the edge in the interior of the disordered chain. Negative rates of variation of the wave functions at the band edges, depending quadratically on the distance, have been found previously for completely uncorrelated Gaussian site energies.[1] Finally we also note that, to leading order in N^{-1}, the rates $\langle \gamma_N^{(2)} \rangle$ at the even and odd sites of a given dimer coincide.

B. Trimer model

In this case the rates of exponential variation of wave functions are given, for the various types of sites, by (26a)–(26c). For intermediate energies we consider the asymptotic limit ($N \to \infty$) of these expressions given by

$$\langle \gamma^{(2)} \rangle = -\frac{\epsilon_0^2 a}{6}\left[2+a+a^2+(1+a)(1+6a+3a^2+a^3) + \frac{a(1+a+a^2)^2}{(a-1)^2}-\frac{a}{a-1}(1+4a+9a^2+4a^3+a^4)\right], \tag{42}$$

whose real and imaginary parts are easily obtained, using (14), e.g.,

$$\mathrm{Re}\langle \gamma^{(2)} \rangle = -\frac{\epsilon_0^2}{6}[2\cos 2q+\cos 4q+\cos 6q+7\cos 8q+9\cos 10q+4\cos 12q+\cos 14q + (4\sin^2 q)^{-1}(\cos 12q+3\cos 10q+5\cos 8q-5\cos 6q - 3\cos 4q-\cos 2q)+(4\sin^2 q)^{-2}(\cos 12q-2\cos 6q+1)], \tag{43}$$

which defines the inverse localization length at the above intermediate energies. The rates $\mathrm{Re}\langle \gamma^{(2)} \rangle$ and $\mathrm{Im}\langle \gamma^{(2)} \rangle$ are plotted as functions of the energy band wave number in Figs. 1 and 2. Figure 1 shows several remarkable features.

(i) The trimer model leads to six delocalized states corresponding to zeros of $\mathrm{Re}\langle \gamma^{(2)} \rangle$ which are symmetrically placed at $q=0.15\pi$, 0.26π, 0.43π, 0.57π, 0.74π, 0.85π, well in the domains of intermediate energies.

(ii) The energies of the delocalized states separate domains of positive values of $\mathrm{Re}\langle \gamma^{(2)} \rangle$, which correspond to true localized states, from domains where

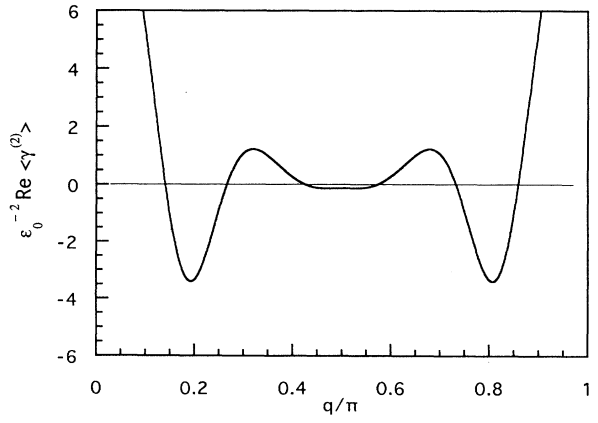

FIG. 1. Reduced inverse localization length vs the pure band energy for the 1D random trimer lattice in contact with an ordered lattice.

FIG. 2. Imaginary part of the Lyapunov exponent vs the pure band energy for the 1D random trimer lattice in contact with an ordered lattice.

$\mathrm{Re}\langle\gamma^{(2)}\rangle$ is negative, which we refer to as domains of *antilocalized states*. The antilocalized states correspond to incident Bloch waves which decrease exponentially away from the edge site towards the interior of the disordered chain. From Fig. 1 it would appear that both types of states (localized and antilocalized) are present in numbers of order N in the energy band, although a more precise statement on their relative distribution would require a study of the density of states.

(iii) From the discussion of Sec. II it is clear that (43) is invalid near the special energies (27) where the weak disorder expansion ceases to be valid for $N\to\infty$. Thus the extrapolations of (43) at the special energies (27) shown in Fig. 1 are of interest only as reference values for measuring the relative importance of the anomalies of $\langle\gamma_N^{(2)}\rangle$ (for finite N) at the special energies studied below. We recall that Eq. (43) for intermediate energies is valid to leading order at finite $N\gg 1$. Figure 2 reveals an interesting antisymmetric variation across the energy band (4) of the additional phase of the wave functions induced by the disorder.

We now study the anomalous forms of $\langle\gamma_N^{(2)}\rangle$ for finite distances N at the special energies (27), by explicitly evaluating (26a)–(26c). At the band center they are readily obtained by inserting the values $a=-1$, $S_M^{(3)}=\frac{1}{2}[1-(-1)^M]$, and $S_M^{(6)}=1$. Similarly, their evaluation at the energies $E=\pm 1$ just requires inserting the solutions $a_\pm=\frac{1}{2}(-1\pm i\sqrt{3})$ (where the upper and lower signs correspond to $E=1$ and to -1, respectively) of $a^2+a+1=0$, for which $a^3=1$ and hence $S_M^{(3)}=S_M^{(6)}=M$. On the other hand, the determination of the rates $\langle\gamma_{3M}^{(2)}\rangle$ and $\langle\gamma_{3M-1}^{(2)}\rangle$ at the energies $E=\pm\sqrt{3}$ corresponding to the solution $a_\pm=\frac{1}{2}(1\pm i\sqrt{3})$ requires expanding the numerator in the quantity $(S_M^{(3)}-S_M^{(-3)})/(a^2-a+1)$ to linear order near $a=a_\pm$, in order to remove its indeterminacy at $a_\pm$. The remaining terms in (26b) and (26c) as well as (26a) are evaluated at $E=\pm\sqrt{3}$ by inserting the values $a=\frac{1}{2}(1\pm i\sqrt{3})$, $S_M^{(3)}=\frac{1}{2}[1-(-1)^M]$, $(a^3=-1)$, and $S_M^{(6)}=M$. Finally, we obtain $\langle\gamma_N^{(2)}\rangle$ at the band edges, by inserting the values $a=1$ and $S_M^{(3)}=S_M^{(6)}=M$ in (26a)–(26c) after performing the necessary power series expansions near $a=1$ in order to remove indeterminacies at $a=1$. This leads successively to the following anomalous rates at the energies (27), at finite distances:

$$\langle\gamma_{3M+1}^{(2)}\rangle=\frac{\epsilon_0^2}{12}\frac{1}{1+(3M)^{-1}}\left[1+\frac{3}{2M}[1-(-1)^M]\right], \tag{44a}$$

$$\langle\gamma_{3M}^{(2)}\rangle=\frac{\epsilon_0^2}{12}\left[1-\frac{3}{2M}[1-(-1)^M]\right], \tag{44b}$$

$$\langle\gamma_{3M-1}^{(2)}\rangle=\frac{\epsilon_0^2}{12}\frac{1}{1-(3M)^{-1}}\left[1-\frac{1}{2M}[1+3(-1)^M]\right], \quad E=0, \tag{44c}$$

$$\langle\gamma_{3M+1}^{(2)}\rangle=-\frac{1}{3}\frac{\epsilon_0^2}{1+(3M)^{-1}}\left[1\mp i\frac{\sqrt{3}}{2}\right], \tag{45a}$$

$$\langle\gamma_{3M}^{(2)}\rangle=\frac{\epsilon_0^2}{3}\left[1\pm i\frac{\sqrt{3}}{2}\right], \tag{45b}$$

$$\langle\gamma_{3M-1}^{(2)}\rangle=\frac{\epsilon_0^2}{3}\frac{1}{1-(3M)^{-1}}\left[2\pm\frac{i3\sqrt{3}}{2}-\frac{1}{4M}(1\pm i\sqrt{3})\right], \tag{45c}$$

where the upper sign corresponds to $E=1$ and the lower sign to $E=-1$ and

$$\langle\gamma_{3M+1}^{(2)}\rangle=\frac{\epsilon_0^2}{12}\frac{1}{1+(3M)^{-1}}\left[13\pm i5\sqrt{3}+(15\mp i11\sqrt{3})\frac{1}{2M}[1-(-1)^M]\right], \tag{46a}$$

$$\langle\gamma_{3M}^{(2)}\rangle=[1+(3M)^{-1}]\langle\gamma_{3M+1}^{(2)}\rangle\pm i\frac{2\sqrt{3}}{3}\epsilon_0^2\left[1+\frac{1}{M}[1-(-1)^M]\right], \tag{46b}$$

$$\langle\gamma_{3M-1}^{(2)}\rangle=[1-(3M)^{-1}]\langle\gamma_{3M}^{(2)}\rangle \mp\frac{i2\sqrt{3}}{3}\frac{\epsilon_0^2}{1-(3M)^{-1}}\left[1+\frac{(-1)^M}{M}-\frac{5}{8M}\left[1\pm\frac{i\sqrt{3}}{3}\right]\right], \tag{46c}$$

where the upper sign corresponds to the results for $E=-\sqrt{3}$ and the lower sign to those for $E=\sqrt{3}$, and finally

$$\langle\gamma_{3M+1}^{(2)}\rangle=-\frac{\epsilon_0^2}{2}\frac{M^2}{1+(3M)^{-1}}\left[9+\frac{1}{2M}-\frac{5}{6M^2}\right], \tag{47a}$$

$$\langle\gamma_{3M}^{(2)}\rangle=[1+(3M)^{-1}]\langle\gamma_{3M+1}^{(2)}\rangle+\frac{\epsilon_0^2}{2}\left[9M+\frac{19}{3}\right], \tag{47b}$$

$$\langle\gamma_{3M-1}^{(2)}\rangle=[1-(3M)^{-1}]\langle\gamma_{3M}^{(2)}\rangle+\frac{\epsilon_0^2}{2}\frac{1}{1-(3M)^{-1}}\left[9M-\frac{8}{3}-\frac{13}{3M}\right], \tag{47c}$$

at the band edges $E=\pm 2$.

The above results lead to the following general observations.

(i) At the band center the rates of localization of wave functions at finite distance are the same, to leading order in N^{-1}, for the three sites of a trimer, unlike in the case of dimer correlations. They are quite different from the extrapolated value obtained from (43).

(ii) At the special energies $E=\pm 1$ the real parts of the rates of variation of the wave functions are different for the three sites of a trimer while being equal at the energies $E=\pm\sqrt{3}$.

(iii) At the band edges the rates are negative and vary quadratically with N for $N\gg 1$, like in the dimer case. As discussed in Sec. III A, this implies antilocalization of the wave functions at the band edges, at nonasymptotic length scales. Note also that, to leading order in N^{-1}, these negative rates are the same for the three types of sites.

C. Monomer-dimer model

The explicit analysis of (33) in the asymptotic domain, for intermediate energies is analogous to that for the random trimer model above. For energies which differ from the special values (27) we have $|a|<1$ in which case we obtain to leading order

$$\langle\gamma^{(2)}\rangle=-\frac{\epsilon_0^2 a}{6}\left[a^3+5a^2+5a+3-\frac{a}{a-1}\left[2a^3+8a^2+7a+3+\frac{2a^2}{a^4+a^2+1}\right]+\frac{a^2}{(a-1)^2}(a^3+3a^2+2a-1)\right], \tag{48}$$

after some analytical manipulations aimed at cancelling the unpleasant denominators, a^6-1, as much as possible. The real part of $\langle\gamma^{(2)}\rangle$ is of special interest since it defines the inverse localization length. Its explicit expression is

$$\mathrm{Re}\langle\gamma^{(2)}\rangle=-\frac{\epsilon_0^2}{6}\left[\cos 8q+5\cos 6q+5\cos 4q+3\cos 2q+\frac{1}{4\sin^2 q}\left[2\cos 10q+6\cos 8q-\cos 6q-4\cos 4q-3\cos 2q+2\frac{\cos 8q-\cos 6q+\cos 4q-2\cos 2q+1}{1+4\cos 4q+4\cos^2 4q}\right]+\frac{1}{16\sin^4 q}(\cos 12q+\cos 10q-3\cos 8q-2\cos 6q+4\cos 4q-\cos 2q)\right], \tag{49}$$

which is plotted in Fig. 3. For completeness sake we also display $\mathrm{Im}\langle\gamma^{(12)}\rangle$ in Fig. 4. An interesting feature of the results of Fig. 3 is the fact that, except for the neighborhood of the special energies $E=\pm\sqrt{3}$, $(q=\pi/6,5\pi/6)$ (where our weak disorder results are anyway invalid for $N\to\infty$) they are remarkably similar to those obtained in Fig. 1 for the trimer model. Indeed $\mathrm{Re}\langle\gamma^{(2)}\rangle$ has six zeros corresponding to extended states at the wave numbers $q\simeq 0.19\pi$, $q\simeq 0.31\pi$, $q\simeq 0.44\pi$, $q\simeq 0.56\pi$, $q\simeq 0.69\pi$, and $q\simeq 0.81\pi$, which are qualitatively similar to those corresponding to extended states in the trimer model. Again the energies of the extended states separate

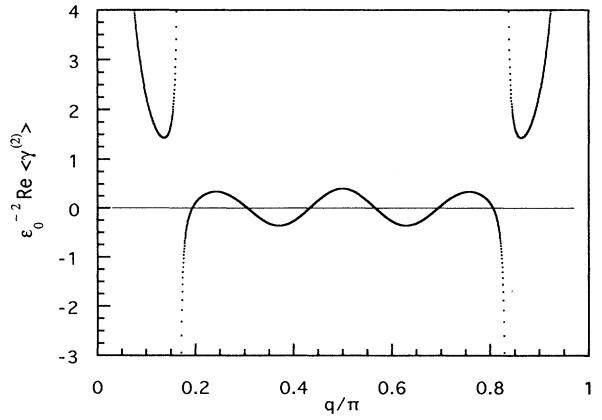

FIG. 3. Same as Fig. 1 for the 1D random dimer-monomer lattice.

FIG. 4. Same as Fig. 2 for the 1D random dimer-monomer lattice.

domains where all states are localized from domains where they are all antilocalized. Apart from the differences between Figs. 1 and 3 in the vicinity of the values $E=\pm\sqrt{3}$, the most significant qualitative difference seems to be that the states in the central region of the energy band are localized for the random monomer-dimer model while being antilocalized for the random trimer model.

The discussion of the rate of wave-function variation at finite distances, Eq. (33), for special energies (27) is simple only for the band center. In this case the analysis is the same as for the trimer model and we obtain

$$\langle \gamma_{3M+1}^{(2)} \rangle = \frac{\epsilon_0^2}{12} \frac{1}{1+(3M)^{-1}} \left[1+\frac{3}{2M}[1-(-1)^M] \right], \quad E=0, \tag{50}$$

which differs from (44a) only by the sign of the second term in the bracket. At each one of the other special energies (27) several terms in (33) are indeterminate and their treatment requires rather lengthy algebra. These results will be discussed in our later publication along with the study of the rates $\langle \gamma_N^{(2)} \rangle$ at the other sites ($N=3M$ and $N=3M-1$) of a monomer-dimer unit and that of their energy dependences in neighborhoods of the special energies.[16]

IV. CONCLUDING REMARKS

In this paper we have studied the influence on one-dimensional (1D) localization of simple correlations of the random tight-binding site energies associated with various multimer systems in contact with an ordered lattice. While previous work on 1D random dimer models has been restricted to a discrete double-valued distribution of site energies we have considered the general case of a continuous distribution.

We have calculated localization lengths at intermediate energies of the pure system's energy band, i.e., energies away from the special values (23) and (27) for the random dimer model and for the random trimer and dimer-monomer models, respectively. At these energies all eigenstates are localized for the random dimer model while, both for the random trimer and for the random dimer-monomer models we have found six delocalized states. More importantly, the delocalized states are found to separate energy domains corresponding to two distinct types of localized states: the usual localized states centered at sites in the interior of the disordered chain and a new type of states which are localized at the contact with the nondisordered lattice, which we have called antilocalized states.

The above results for the inverse localization length for weak disorder (i.e., random site energies small compared to the nearest-neighbor hopping rate) cannot be directly compared with the results of Dunlap *et al.*[4] for a random dimer model defined from a binary alloy lattice with randomly distributed constituents having fixed energies ϵ_A and ϵ_B. The random alloy model closest to our lattice with Gaussian site energies fluctuating weakly about an ordered energy level (at $E=0$), would correspond to the case of arbitrarily small energy differences, $\epsilon_A-\epsilon_B$, for the constituents, e.g., $\epsilon_A=w$, $\epsilon_B=-w$, $w\to 0$, where both ϵ_A and ϵ_B would be assigned to lattice sites with probabilities of $\frac{1}{2}$ (equiconcentrated alloy). In this case ϵ_A and ϵ_B could indeed be viewed as small fluctuations (with a vanishing mean) about a fictitious nondisordered atomic level at $E=0$. This random alloy lattice should further be in contact with an ordered semi-infinite lattice with site energies $\epsilon=0$ (rather than with an ordered parent alloy lattice with alternating site energies ϵ_A and ϵ_B). Clearly the weak disorder expansion in powers of site-energy fluctuations applied to this random alloy model, generalized to include the dimer correlations of Sec. II, could not reveal the now familiar delocalization of states for *finite* large values of the site energies difference, namely $\epsilon_A-\epsilon_B=\pm 2V$, where V is the constant nearest-neighbor hopping rate.[4] We recall that the purpose of this paper was to present an analysis of the localization problem (and of delocalization of states, in particular) specifically for weakly disordered multimer models in contact with an ordered lattice, using a method akin to the familiar weak disorder expansions for Anderson localization in the case of uncorrelated random site energies (see Ref. 1 and references therein).

Another remark concerns the existence of different types of random dimer and trimer models. In Sec. II, we have restricted ourselves to models in which the random site energies are individually assigned to pairs or triplets of lattice sites in succession. It seems reasonable to assume that randomness in these systems (which divide up into independent fluctuating unit cells with two sites per cell) is maximal[4] with respect to cases where only a fraction of the sites are grouped into pairs whose constituent nearest-neighbor sites are assigned common energies fluctuating independently from one pair to another, while the remaining sites are assigned independently fluctuating energies. Our random dimer-monomer model which leads to delocalized states at energies corresponding to localization-antilocalization transitions (Fig. 3) is a special model of this type. The appearance of localization-antilocalization transitions and of associated delocalized states might, in fact, be expected to be a common feature of these generalized dimer models, which would contrast with the simple dimer model of Sec. II, where all states are localized. In this context we also recall that in the random dimer model of Dunlap *et al.*[4] delocalized states have been found numerically in the case where one of the two site energies (ϵ_A or ϵ_B) is assigned at random to pairs of lattice sites, as well as in the case where both site energies are individually assigned to pairs of sites in succession.

The antilocalized states are expected to play a special role, e.g., in the study of the electrical noise associated with the scattering of electrons by the surface of a disordered conductor. Here the overlap of incident electrons with Anderson localized states near the surface of the conductor causes random delays in the electron backscattering, leading to a low-frequency current fluctuation noise.[17,18]

We have also studied the rates of exponential variation of the site wave functions at the above special energies for

finite distances from the edge site. As discussed earlier[1] for the monomer model (i.e., for completely uncorrelated site energies) these results may be used for discussing the resistance of metallic samples of length $N \ll \xi$ (localization length). Indeed, the Landauer formula[19] relates the resistance to the transmission coefficient $\langle |t_N|^2 \rangle$ which in turn is expected to be given by

$$\langle |t_N|^2 \rangle \sim \exp[-2|\mathrm{Re}\langle \gamma_N \rangle|N] \ .$$

ACKNOWLEDGMENT

I am grateful to Dr. J. Schmit for help with the numerical calculations.

[1] J. Heinrichs, Phys. Rev. B **50**, 5295 (1994).

[2] D. J. Thouless, in *Ill-Condensed Matter,* edited by R. Balian, R. Maynard, and G. Toulouse (North-Holland, Amsterdam, 1979).

[3] D. H. Dunlap, K. Kundu, and P. Phillips, Phys. Rev. B **40**, 10 999 (1989).

[4] D. H. Dunlap, H.-L. Wu, and P. W. Phillips, Phys. Rev. Lett. **65**, 88 (1990).

[5] J. C. Flores, J. Phys. Condens. Matter **1**, 8471 (1989).

[6] H.-L. Wu and P. Phillips, Phys. Rev. Lett. **66**, 1366 (1991).

[7] H.-L. Wu, W. Goff, and P. Phillips, Phys. Rev. B **45**, 1623 (1992).

[8] S. N. Evangelou and A. Z. Wang, Phys. Rev. B **47**, 13 126 (1993).

[9] P. K. Datta, D. Guri, and K. Kundu, Phys. Rev. B **48**, 16 347 (1993).

[10] A. Bovier, J. Phys. A **25**, 1021 (1992).

[11] S. Sil, S. N. Karmakar, R. K. Moitra, and A. Chakrabarti, Phys. Rev. B **48**, 4192 (1993).

[12] S. N. Evangelou and E. N. Economou, J. Phys. A **26**, 2803 (1993).

[13] A. Sanchez and F. Dominguez-Adame, J. Phys. A **27**, 3725 (1994).

[14] M. Kappus and F. Wegner, Z. Phys. B **45**, 15 (1981).

[15] B. Derrida and E. J. Gardner, J. Phys. (Paris) **45**, 1283 (1984).

[16] J. Heinrichs (unpublished).

[17] J. B. Pendry, P. D. Kirkman, and E. Castano, Phys. Rev. Lett. **57**, 2983 (1986).

[18] J. Heinrichs, J. Phys. Condens. Matter **2**, 1559 (1990).

[19] R. Landauer, Philos. Mag. **21**, 863 (1970).